Effect of Molecular Size of Pegylated Peptide on the Pharmacokinetics and Tumor Targeting in Lymphoma-Bearing Mice[1]

Sally J. DeNardo,[2] Zhengsheng Yao, Kit S. Lam, Aimin Song, Patricia A. Burke, Gary R. Mirick, Kathleen R. Lamborn, Robert T. O'Donnell, and Gerald L. DeNardo

Department of Internal Medicine, Division of Hematology/Oncology, Section of Radiodiagnosis and Therapy, University of California Davis Medical Center, Sacramento, California 95816 [S. J. D., Z. Y., P. A. B., G. R. M., R. T. O., G. L. D.]; Department of Internal Medicine, Division of Hematology/Oncology, University of California, Davis Medical Center, Sacramento, California 95817 [K. S. L., A. S.]; and Brain Tumor Research Center, University of California San Francisco, San Francisco, California 94143 [K. R. L.]

Abstract

Purpose: **Rapid blood and body clearances have hampered effective tumor targeting by small molecules. We used branched poly(ethylene glycol) (pegylated) polymers (M_r 40,000, M_r 70,000, M_r 100,000, and M_r 150,000) conjugated to tumor-specific and control peptides to assess the effect of both molecular weight and tumor specificity on pharmacokinetics and biodistribution.**

Experimental Design: **Pegylated specific lymphoma-binding peptide and control peptide (containing stereoisomers of proline and aspartate) were synthesized, radiolabeled with ^{111}In, fractionated by size, and injected into Raji lymphoma-bearing athymic mice (4–6 mice/group). Pharmacokinetics were followed for 2 days to evaluate effects of specificity and molecular size on blood clearance, body clearance, and biodistribution.**

Results: **As molecular size increased, blood and body clearances decreased ($P < 0.001$). The effect of molecular size on blood clearance was not altered by ligand binding specificity ($P = 0.21$), with $t_{1/2}$ ranging from 5.4 h (M_r 40,000) to 17.7 h (M_r 150,000). However, ligand specificity did alter body clearance, with pegylated control peptides clearing the body more slowly than pegylated specific peptides [$P = 0.03$; range, 19.1–91.3 h (specific peptides) *versus* 23.6–115.7 h (control peptides)]. At 24 h, there was more uptake of specific *versus* control pegylated peptides in tumor, liver, and marrow, but there was less uptake in kidneys, with a more pronounced difference for the higher molecular weight peptides ($P < 0.01$).**

Conclusions: **These results demonstrate that the pharmacokinetics and biodistribution of peptides and resultant uptake in tumor and normal tissues can be altered by both molecular size and ligand specificity, with molecular size affecting pharmacokinetics and organ uptake in a predictable manner.**

Introduction

Radiolabeled peptides that specifically target malignant tissues provide new options for cancer detection and therapy. Antitumor monoclonal antibodies, as well as single chain antibodies, conjugated to radiometals, are currently used to target tumors (1–8). However, monoclonal antibodies, because of their large size (M_r 160,000), typically do not effectively penetrate the entire tumor (9–11). Single chain antibodies (M_r 25,000), although much smaller than monoclonal antibodies, tend, like monoclonal antibodies, to be taken up in tissues "processing" protein, leading to dose-limiting toxicities (12, 13). Lam and co-workers (14–16), using the one-bead one compound approach, have developed a library of lymphoma targeting peptides. Using this approach, several peptide ligands that bind preferentially to malignant human T- and B-lymphoma cell lines were identified (16, 17). These peptides, like scFv,[3] may have normal tissue uptake and, as small molecules, unless modified, are cleared too rapidly to effectively deliver tumor therapy (18, 19).

Pegylation, the covalent attachment of PEG polymers to peptides, cytokines, and enzymes (20–24), delays the elimination of these pharmaceuticals from the circulation by a variety of mechanisms, including decreasing renal clearance, proteolysis, and immunogenicity (25–28). Accordingly, PEG-based modifications have been used to prolong circulation time and hence bioavailability of smaller antibody-based agents such as Fab fragments, scFv fragments (linked variable heavy and light chains), and peptides (23, 25, 26, 28–33). Pegylation inhibits

[1] Presented at the "Ninth Conference on Cancer Therapy with Antibodies and Immunoconjugates," October 24–26, 2002, Princeton, NJ. This work was supported by California Cancer Research Program Contract 00-00764V-20133, NIH Grant R33 CA89706-01, Department of Energy Grant DE-FG03-84ER60233, and National Cancer Institute Grant PO1 CA47829.

[2] To whom requests for reprints should be addressed, at Radiodiagnosis and Therapy, University of California Davis Medical Center, 1508 Alhambra Blvd, Sacramento, CA 95816. Phone: (916) 734-3787; Fax: (916) 451-2857; E-mail: sjdenardo@ucdavis.edu.

[3] The abbreviations used are: scFv, single chain antibody fragment; PEG, poly(ethylene glycol); eq, molar equivalent; HOBt, *N*-hydroxybenzotriazol; DIC, 1,3-diisopropylcarbodiimide; DMF, *N*,*N*-dimethylformamide; TFA, trifluoroacetic acid; *Dhb*, 3,5-dihydroxybenzyl acid; pLDI, D-Pro-L-Leu-L-Asp-L-Ile; PLdI, L-Pro-L-Leu-D-Asp-L-Ile; O*t*-Bu, *tert*-Butoxy; Boc, t-butoxycarbonyl; Fmoc, 9-fluorenylmethoxycarbonyl; DOTA, 1,4,7,10-tetrazacyclododecane-*N*,*N*′,*N*″,*N*‴-tetraacetic acid; HPLC, high-performance liquid chromatography; %ID, percentage of injected dose; %ID/g, percentage of injected dose per gram of tissue; ANCOVA, analysis of covariance; IL, interleukin; TNF, tumor necrosis factor.

degradation by proteolytic enzymes and, by increasing the apparent molecular size, reduces the rate of renal filtration (23, 25, 34). $F(ab')_2$ fragments attached to linear PEG polymers circulate twice as long as unmodified $F(ab')_2$ fragments, resulting in enhanced tumor localization compared with nonpegylated molecules (35). Pegylated peptides, in addition to increasing molecular size, present an opportunity to devise configurations that optimize tumor delivery and binding through the use of branched structures to enhance binding and avidity (31).

Although some proteins, antibodies, antibody fragments, and other biological materials have been pegylated for specific applications (25, 26, 31–33, 36–42), little is known regarding the effect of variations in the size of PEG on the same tumor-specific PEG-peptide molecules. Linear PEG has been used to increase the effective size of small molecules, with resultant increases in tumor targeting (27, 32, 33, 35, 39, 42–48), but less is known about the effect of size on the pharmacokinetics and organ uptake of small peptides conjugated to branched PEG molecules.

In this study, a lymphoma-specific peptide, $(Dhb\text{-pLDI})_6/(Dhb\text{-pLDIK})_2$PEG (16, 17), and a control peptide, $(Dhb\text{-PLdI})_6/(Dhb\text{-PLdIK})_2$PEG, which were similar except for stereoisomers of two amino acids critical for specific binding to the selected tumor ligand, were prepared and fractionated by size, and their *in vivo* pharmacokinetics and tumor and normal tissue uptake were investigated. Our results demonstrate not only dependence of body and blood clearance on molecular size, with increased uptake by tumor associated with increased circulation time, but also show differences in normal organ uptake related to both peptide sequence and molecular size.

Materials and Methods

Reagents. Branched NH_2-PEG with eight arms was purchased from Shearwater Polymers, Inc. (Huntsville, AL; Ref. 24). All Fmoc-protected amino acids were purchased from SynPep (Dublin, CA). HOBt, DIC, and TFA were purchased from Advanced ChemTech (Louisville, KY). Ethyl ether and DMF were purchased from Aldrich (Milwaukee, WI) and VWR (Brisbane, CA), respectively, and used without purification. Isothiocyanatobenzyl-DOTA was purchased from Macrocyclics (Richardson, TX), and ^{111}In was purchased from Nordion (Kanata, Ontario, Canada).

Peptide Synthesis on PEG. Synthesis and schematic structure of the pegylated peptides are outlined in Fig. 1. Standard Fmoc chemistry was used (49). Two of the eight NH_2 termini of the octavalent-PEG were derivatized with N^{α}Fmoc-N^{ϵ}Boc-lysine [0.25 eq of Fmoc-Lys(Boc)-OH, 0.25 eq of HOBt, and 0.25 eq of DIC in DMF], which were used for later conjugation with the radiometal chelate DOTA. After Fmoc deprotection in 25% piperidine/DMF, the peptide ligand was synthesized directly on the $(NH_2)_6/(Lys(Boc))_2$-PEG scaffold. A typical synthetic procedure is as follows: $(NH_2)_6/(Lys(Boc))_2$-PEG (1.6 g, 0.08 mmol), Fmoc-AA (1.92 mmol, with Fmoc-AA = Fmoc-Pro-OH, Fmoc-D-Pro-OH, Fmoc-Leu-OH, Fmoc-D-Asp(O*t*Bu)-OH, Fmoc-Asp(O*t*Bu)-OH, or Fmoc-Ile-OH), HOBt (294 mg, 1.92 mmol), and DIC (301 μl, 1.92 mmol) were stirred in 5 ml of DMF for 1 h. After this, 25 ml of ethyl ether were added dropwise to the solution at 0°C. The precipitated pegylated peptide was filtered and redissolved in DMF, precipitated with ethyl ether twice, washed with ethyl ether five times, and dried under vacuum. To remove Fmoc, the amino acid-coupled PEG was dissolved in 5 ml of 25% piperidine/DMF, stirred for 1 h, and then precipitated with ethyl ether. The Kaiser test was carried out to monitor amino acid coupling and Fmoc deprotection (50). This cycle was repeated until all desired

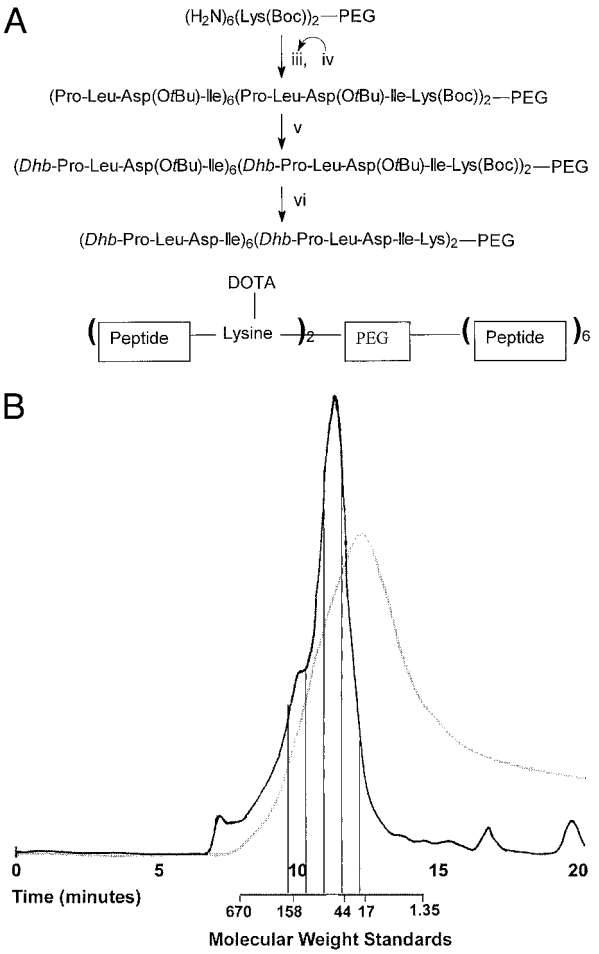

Fig. 1 *A*, synthesis of pegylated peptides. Branched NH_2-PEG with eight arms was used for scaffold for amino acid coupling using standard Fmoc chemistry for the synthesis of lymphoma-binding peptide $(Dhb\text{-pLDI})_6/(Dhb\text{-pLDIK})_2$PEG and control peptide $(Dhb\text{-PLdI})_6/(Dhb\text{-PLdIK})_2$PEG. *i*, 0.25 eq Fmoc-Lys(Boc)-OH, HOBt, DIC; *ii*, 25% piperidine in DMF; *iii*, 3 eq Fmoc-AA, HOBt, and DIC [Fmoc-AA = Fmoc-Ile-OH, Fmoc-Asp(O*t*Bu)-OH or Fmoc-D-Asp(O*t*Bu)-OH, Fmoc-Leu-OH, Fmoc-D-Pro-OH, or Fmoc-Pro-OH]; *iv*, 25% piperidine in DMF; *v*, 3 eq 3,5-dihydroxybenzoic acid, HOBt, and DIC; *vi*, 95% TFA in water. *B*, preparative HPLC separation of size fraction of pegylated peptide. After synthesis, pegylated peptides were centrifuge-filtered to retain molecules between M_r 30,000 and M_r 300,000. After conjugation with DOTA and radiolabeling with ^{111}In, HPLC separation by radioanalytic detection (cpm, shown in *light gray*) and UV detection (280 nm, *dark line*) were used to obtain 0.5-ml fractions. The *trace* shown illustrates the approximate range of molecular weight for each fraction used (indicated by *vertical lines* on protein trace), including M_r 40,000, M_r 70,000, M_r 100,000, and M_r 150,000 fractions. Time is indicated on the bottom of the trace (1 ml/min). Molecular weight standards with their times of elution are indicated *below* the trace.

amino acid coupling was completed and the NH_2 termini of the peptides were capped by *Dhb*. The pegylated peptide was then dissolved in 5 ml of 95% TFA/water and stirred for 2 h to remove side chain protection groups (t-But of Asp and Boc of Lys). The crude pegylated peptide was precipitated with ethyl ether, dialyzed against water, and lyophilized, resulting in 1.5 g of white powder with a yield of 75%. Known concentrations of (*Dhb*-pLDI)$_6$/(*Dhb*-pLDIK)$_2$PEG and (*Dhb*-PLdI)$_6$/(*Dhb*-PLdIK) $_2$PEG were measured by UV absorbance (Beckman DU-64) to determine the extinction coefficient, which was 9.2 for 1% (w/v) solution at 280 nm ($\epsilon^{1\%}{}_{280} = 9.2$). A scheme of the synthesis and final product is shown in Fig. 1*A*. To resolve heterogeneous eight-arm PEG peptide conjugates to a narrow range of molecular size, pegylated peptides were centrifuge filtered (Microsep 300K; Pall Filtration, Northborough, MA), which removed conjugates with an apparent molecular weight of >300,000. Further filtration was done with Centricon 30 filters (Centricon 30; Amicon, Beverly, MA), which removed material with an apparent molecular weight of <30,000.

DOTA Conjugation. For radiolabeling with ^{111}In, the pegylated peptides were first conjugated with DOTA as described previously (51). Pegylated peptide, specific and control [75 nmol in 90 μl-0.1 M tetramethylammonium phosphate (pH 8.5)], was combined with *p*-isothiocyanatobenzyl-DOTA [800 nmol in 32 μl-0.1 M tetramethylammonium phosphate (pH 7)] and 2 M triethylamine (7 μl). The reaction was incubated for 2 h at 37°C. DOTA-pegylated peptide conjugate was purified and transferred to 0.1 M ammonium acetate (pH 5.3) by centrifuged column filtration (52). Both specific and control conjugates had a mean of one metal binding DOTA moiety per eight-armed PEG molecule as determined by cobalt binding assay (53).

^{111}In Radiolabeling. A representative radiolabeling of specific or control PEG conjugate was performed as follows. ^{111}In (4.8 mCi in 12 μl-0.05 M hydrochloric acid) was buffered in 0.4 M ammonium acetate (4 μl). DOTA-(*Dhb*-pLDI)$_6$/(*Dhb*-pLDIK)$_2$ [0.18 mg in 35 μl-0.1 M ammonium acetate (pH 5)] was added. The radiolabeling solution was incubated at 37°C for 15 min. EDTA (0.5 nmol in 5 μl) was added to scavenge unchelated ^{111}In. ^{111}In-DOTA-pegylated peptide (4.2 mCi/0.18 mg) was then purified and transferred to PBS by centrifuged column filtration. The radiopharmaceutical was formulated to a final specific activity of 4 μCi ^{111}In/μg PEG by the addition of pegylated peptide (0.87 mg).

HPLC Size Selection and Analysis. DOTA-conjugated pegylated peptides or their ^{111}In-labeled forms were applied to HPLC (Beckman 332; Beckman, Fullerton, CA) to select molecular species based on size (Fig. 1*B*). HPLC was performed using a gel filtration column (Biosep SEC-S3000; 7.8 × 300 mm; Phenomenex, Torrance, CA) eluted with 0.1 M sodium phosphate buffer/0.1% sodium azide (pH 7), at a flow rate of 1.0 ml/min. Molecular weight standards (Bio-Rad, Hercules, CA) were used to develop standard curves for elution volume as a function of molecular size. Detection was by radioanalytic detection (Beckman 170) and UV absorbance at 280 nm (Beckman 166 detector). Fractions of 0.5 ml each were collected, and the radioactivity was counted. Fractions representing M_r 40,000, M_r 70,000, M_r 100,000, and M_r 150,000 based on molecular weight standards were used in *in vitro* and *in vivo* studies after samples of each fraction were rechromatographed under the same conditions to verify the molecular size profile. Similar analytical HPLC profiles were observed for specific and control peptides when rechromatographed, indicating that similar molecular weight ranges were used for both.

Cell Culture. Raji, a human Burkitt's lymphoma cell line (54), was obtained from the American Type Culture Collection (Manassas, VA). Raji cells were grown and maintained in RPMI 1640 supplemented with 10% FCS, 1 mM sodium pyruvate, and 0.1 mM nonessential amino acids. Viability was determined by trypan blue exclusion before cell binding assays and implantation in mice.

Cell Binding Immunoreactivity Competitive Assay. The appropriate fractions of unlabeled and labeled pegylated peptide were diluted to the desired concentrations in Tris-buffered saline plus 2 mM $MnCl_2$ (pH 7) to maximize binding percentage (55). Labeled pegylated peptide, 10–25 ng (2 mM) in 50 μl, was added to triplicate tubes for each level of competition. Unlabeled pegylated peptides at levels between 0 and 100-fold excess (in 50 μl) were added to the replicates as competitor. Viable cells were diluted to 2×10^7 cells/ml in Tris-buffered saline containing 2 mM $MnCl_2$. One million cells (50 μl) were added to the replicates, vortexed, and incubated for 1 h at room temperature. The cells were pelleted by centrifugation at 300 × *g* for 10 min, and the supernatant and cells were counted. The percentage bound was calculated as follows: [cell bound cpm/(cell cpm + supernatant cpm)] × 100. Scatchard analysis of the competitive binding was used to estimate the affinity constants (K_a; Ref. 56).

Mouse Model. Six-week-old female athymic BALB/c *nu/nu* mice (Harlan Sprague Dawley, Frederick, MD) were maintained on a normal, *ab libitum* diet and under pathogen-free conditions, according to University of California animal care guidelines. Four days before implantation of Raji cells, the mice received external beam radiation (400 rads) to suppress the immune response (54). Raji cells (5.5×10^6) were injected s.c. into both sides of the lower abdomen. Tumors were grown for 20–25 days and measured in three orthogonal diameters using a caliper, and the volume was calculated by the formula for hemiellipsoids (57). Tumor volume at the time of experiment ranged between 50 and 500 mm^3, with a mean tumor volume (±1 SD) of 214 ± 70 mm^3. Mice were sorted by tumor size into experimental groups with 4–6 mice/group, such that all groups had both comparable numbers of similar-sized tumors and similar mean volumes.

Pharmacokinetic Studies. Groups of 4–6 mice, either normal or Raji tumor-bearing mice, received i.v. injections of 750 kBq (20 μCi, 5 μg) of ^{111}In labeled pegylated peptide via tail vein. Total body activities of mice were measured at the time of injection, and at 1 h (and at 2 h for M_r 40,000), 4 h, 24 h, and 48 h after injection, using two opposed, isoresponsive sodium iodide detectors (Canberra Nuclear). The radioactivity in blood was evaluated by taking 2 μl of blood from the tail vein at 5 min, 1 h (and at 2 h for M_r 40,000), 4 h, 24 h, and 48 h after injection, and counting the blood samples in a gamma well counter along with tissues taken for biodistribution (see below). Decay-corrected radioactivity in the total body and blood were expressed as %ID and %ID/ml, respectively. Whole-body and blood clearances, expressed as $t_{1/2}$, were determined from the regression line slopes obtained by plotting ln %ID *versus* time

Table 1 Binding of specific and control ^{111}In-labeled pegylated peptides to Raji cells

Analysis of cell binding (% bound) was compared for specific and control pegylated peptides using unlabeled competitor pegylated peptide. For binding of specific pegylated peptide, both unlabeled specific peptide and unlabeled control peptide of similar molecular weights were used as competitor peptides. For binding of control peptide, only unlabeled specific peptide was used as competitor. Scatchard analysis was used to estimate affinity constants (K_a). Approximately 25–28% of binding of specific peptide could not be blocked using cold specific peptide, consistent with nonspecific binding or internalization of peptide. Binding of control peptide was not blocked by competition with specific peptide and was only slightly lower than binding of similarly sized specific peptides, consistent with recognition of different cell surface sites by specific and control peptides.

	M_r (thousands)	Mean % bound ± SD (no competitor)	Mean % bound ± SD (competitor used)		K_a (10^8 M^{-1})
			Specific	Control	
Specific	40	60 ± 6	27 ± 3		1 ± 0.3
	70	64 ± 4	25 ± 2		1 ± 0.2
	100	67 ± 4	28 ± 2		2 ± 0.3
	100	49 ± 5		52 ± 5	
	150	49 ± 2		51 ± 4	
Control	100	46 ± 6	43 ± 3		
	150	38 ± 9	42 ± 1		

for each mouse. Blood clearance rates were calculated using a single regression line to obtain a single clearance rate because insufficient early data points were available for statistical analysis of both α and β clearances.

To assess the biodistribution of ^{111}In-pegylated peptides, the mice were sacrificed by cervical dislocation at 1 and 2 days after injection. Tumors and normal tissues were harvested and weighed, and blood samples, organs, and tumors were counted in a sodium iodide gamma well counter (Packard, Downers Grove, IL). Counts were calibrated using ^{111}In standards in the appropriate sample configuration and volumes. The decay-corrected concentrations of radioactivity in tumors and normal tissues were expressed as %ID/g.

Statistics. Radioactivity from body, blood, tumor, and normal organs was calculated for each mouse. To evaluate differences in body and blood clearance rates between animals and then between groups, the rate of clearance was estimated for each animal by determining the slope of the regression line for the ln %ID *versus* time in hours. These blood and body regression line slopes were used to obtain $t_{1/2}$ in hours for each mouse for both blood and body clearance. Differences (of slope) between the specific and control agents and the effect of increasing molecular size were assessed using ANCOVA between groups. Initially, the model was fit with the following variables: specific *versus* control; molecular size; and a term for the interaction between the two. In this model, the assumption is made that the clearance rates will change linearly as a function of the molecular weight. If the interaction was significant, this implied that the impact of the increasing molecular size on the clearance differed, depending on whether the specific or control pegylated peptide was used. If that was the case, the clearance rates as a function of molecular weight were estimated separately for the two groups. If the interaction had a $P \geq 0.1$, then a model was fit without the interaction term (reduced model), and both the estimate of the impact of specific *versus* control and the effect of increasing molecular size were estimated from this reduced model.

Analysis of organ and tumor uptake was done in a comparable fashion but used the %ID/g from each mouse at either 24 or 48 h. First, an ANCOVA model was fit including terms for specific *versus* control pegylated peptide, molecular size, and the interaction. If the *P* for the interaction was ≥0.1 then the reduced model, with no interaction term, was used. Otherwise, the uptake was estimated separately for specific and control pegylated peptide.

All *P*s presented are two-tailed analyses, with results considered statistically significant if *P* was <0.05.

Results

Cell Binding Studies. The radiolabeled pegylated tumor-specific peptides had 49–67% binding to Raji cells *in vitro* (Table 1). The percentage bound were challenged by addition of the same specific unlabeled pegylated peptide molecules as competitor. Scatchard analysis of 0–100-fold excess competitor resulted in estimated binding affinities for the specific pegylated peptide molecules of 10^8 M^{-1}. Approximately 25–28% of binding of specific pegylated peptide could not be blocked using cold specific peptide, consistent with nonspecific binding or internalization of peptide. Binding studies done under low-temperature conditions were not performed, thus it is not clear how much specific binding, which could not be blocked, is due to internalization. Control pegylated peptide molecules did not reduce binding of specific pegylated peptides. Binding of the control peptide (38–46% binding), done with the larger (M_r 100,000–150,000) pegylated peptides, was only slightly lower than binding of similarly sized specific peptides (49%) and could not be blocked by competition with specific peptide, demonstrating that these specific and control pegylated peptides recognize different molecular sites on the cell surface.

Blood and Body Clearance. Blood clearance, estimated by the slope of the regression line from each mouse (ln % ID *versus* time), was reduced as molecular size of pegylated peptide increased for both specific and control peptides, and the extent of reduction (interaction term) was not statistically significant ($P = 0.21$; Fig. 2). Because the interaction was not significant, analysis using the reduced statistical model was used. This analysis showed a definite effect of molecular size on blood

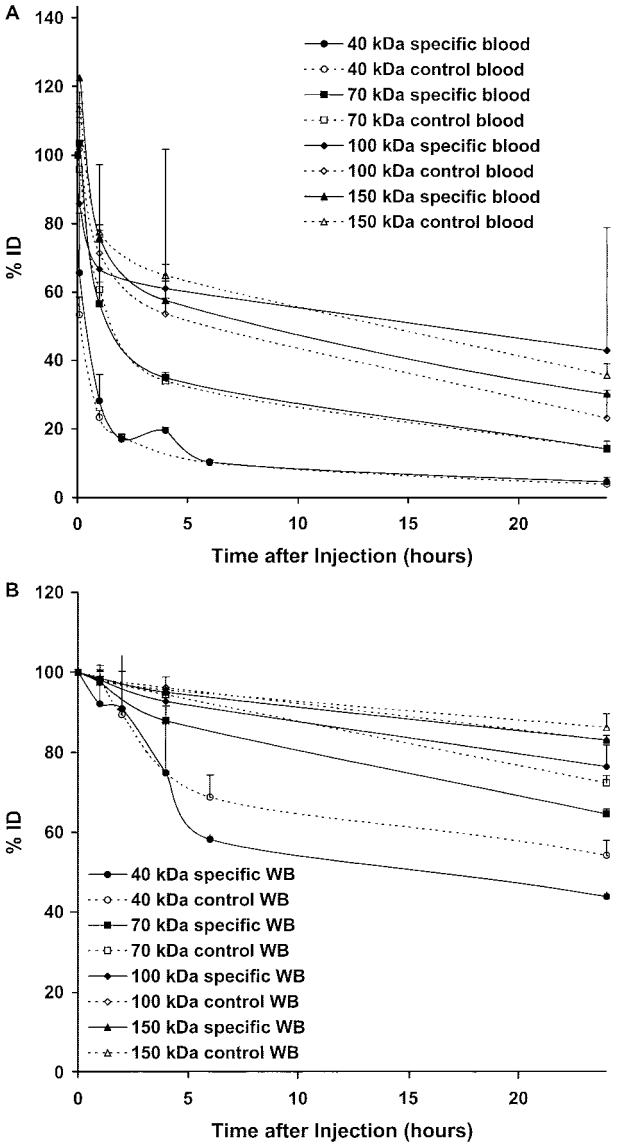

Fig. 2 Blood and body clearance of specific and control pegylated peptides. Clearances of radioactivity (mean %ID ± SD *versus* time) for (*A*) blood and (*B*) body are shown as linear plots. Clearance rate [calculated as the change in the ln %ID/time (h)] of blood was not different for specific *versus* control pegylated peptides (*A*), but the body clearance rate was faster for specific pegylated peptides (*B*; see Table 2 for specific clearance rates expressed as $t_{1/2}$). Both blood and body clearance rates were dependent on molecular weight ($P < 0.001$). Specific clearances are indicated by *solid lines* and *filled symbols*, and control clearances are indicated by *dotted lines* and *open symbols*. These results illustrate that the circulation and retention times of pegylated peptides were controlled by molecular size.

clearance ($P < 0.001$), but no difference in blood clearance between the specific and control peptides of the same size ($P = 0.42$). Estimated α (using time 0 to 1 h) and β clearance (using 1–24 h) rates for blood demonstrated the same trend as found by analysis using a single regression line, with no effect of specificity on either phase (data not shown). For example, blood clearance rates ($t_{1/2}$ in hours) for M_r 150,000 pegylated peptides

Table 2 Blood and body clearances

Blood and body clearances were determined by plotting the In %ID *versus* time for each mouse. A rate of clearance (slope) was obtained by regression analysis, which was used to calculate the $t_{1/2}$ in hours. The mean $t_{1/2}$ ± SD is shown for each group of mice at each molecular weight (in thousands). Statistical analysis (using the slopes) indicated that blood clearance was not affected by specificity ($P = 0.21$) but decreased with molecular weight ($P < 0.001$). Body clearances were affected by specificity ($P = 0.03$), with faster clearance occurring with specific peptides. Slower body clearances for both specific and control pegylated peptides were associated with increased molecular weight ($P < 0.001$).

	Peptide	M_r (in thousands)	Mice/group	Mean $t_{1/2}$ (h)	SD
Blood	Specific	40	11	5.4	0.8
	Control	40	6	5.7	1.4
	Specific	70	5	8.0	0.6
	Control	70	4	7.9	0.3
	Specific	100	9	10.8	36.7[a]
	Control	100	7	11.0	2.4
	Specific	150	4	17.7	0.8
	Control	150	5	15.5	2.4
Body	Specific	40	11	19.1	0.8
	Control	40	6	23.6	1.9
	Specific	70	5	37.3	1.8
	Control	70	4	51.4	4.3
	Specific	100	9	60.8	3.5
	Control	100	7	96.7	33.2[a]
	Specific	150	4	91.3	4.7
	Control	150	5	115.7	30.0[a]

[a] High SD in these clearance values resulted from variability in mouse data.

were 17.7 ± 0.8 h for specific peptide and 15.5 ± 2.4 h for control peptide, whereas blood clearance rates for M_r 70,000 pegylated peptides were 8.0 ± 0.6 h for the specific peptide and 8.0 ± 0.3 h for the control peptide (Table 2). Thus the decrease in clearance in blood with increasing molecular size was similar for specific and control peptides. The changes in clearance with size and the similar clearances for specific and control peptides were consistent with the selection of definitive size ranges of pegylated peptides for use in this study. For body clearance, the change in clearance due to molecular size was dependent on specificity of peptide ($P = 0.03$; Fig. 2; Table 2). For example, the rate of body clearance for specific pegylated peptide was 37.3 ± 1.8 h (M_r 70,000), 60.8 ± 3.5 h (M_r 100,000), and 91.3 ± 4.7 h (M_r 150,000), whereas the apparently slower clearance rates for the control pegylated peptide were 51.4 ± 4.3 (M_r 70,000), 96.7 ± 33.2 h (M_r 100,000), and 115.7 ± 30.0 h (M_r 150,000). Thus the rate of body clearance for the control pegylated peptides decreased with increasing molecular size at a different rate than for specific pegylated peptides. Both of these rate changes (specific and control) were statistically significant ($P < 0.001$). Both the HPLC analysis and the similar rates observed for blood clearance indicate that specific and control peptides were similarly sized. Thus the data indicate that specific and control peptides of similar sizes behave differently as determined by body clearances.

Biodistribution in Normal Organs and Tumor: Effect of Specificity. Organ uptake was evaluated for tumor, blood, kidney, liver, spleen, and marrow at 24 and 48 h after injection

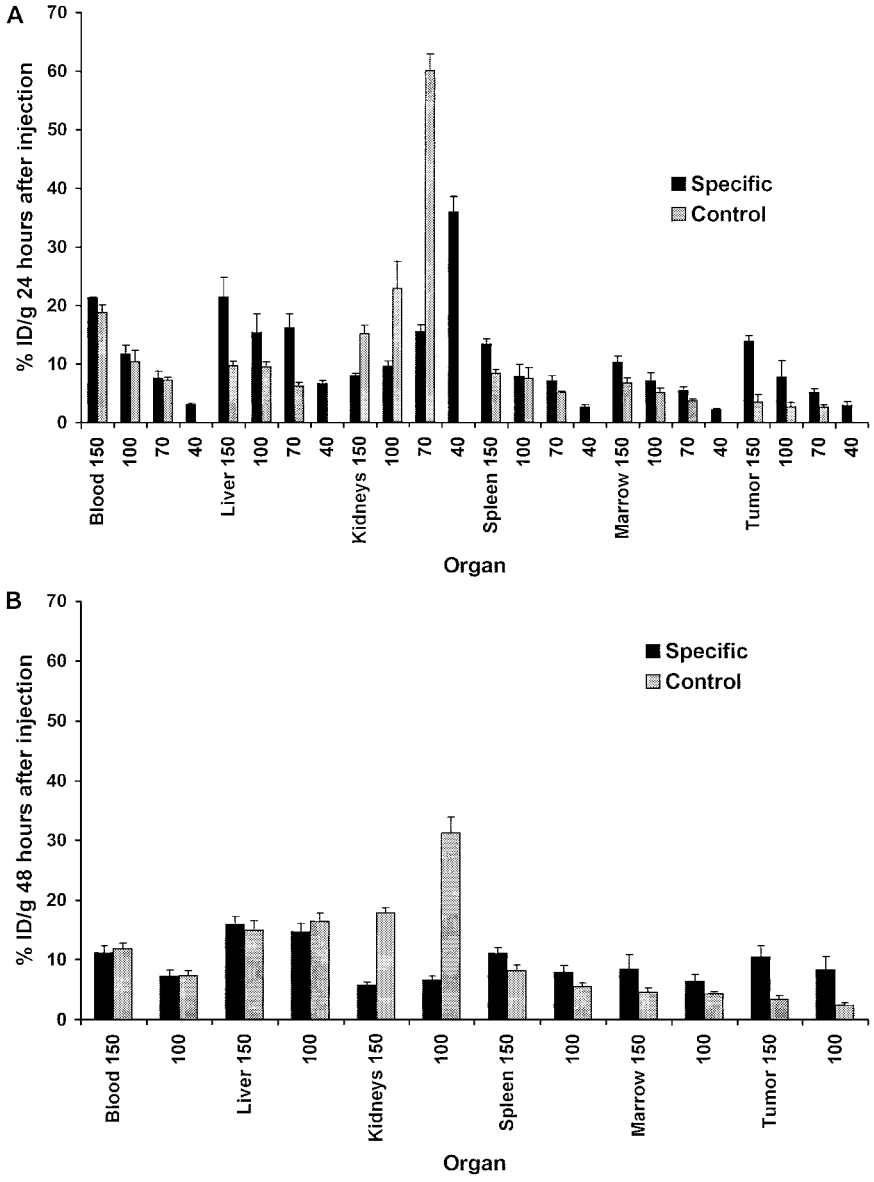

Fig. 3 Organ uptake of specific and control pegylated peptides. The %ID/g was determined for specific and control pegylated peptides in blood (%ID/ml), liver, kidneys, spleen, marrow, and tumor from mice sacrificed (*A*) 24 and (*B*) 48 h after injection of radiolabeled peptides. The mean size of tumors at the time of injection was 214 ± 70 mm^3. Specific organ uptake is indicated by *black bars*, and control uptake is indicated by *gray bars* (M_r 40,000 control peptide was not evaluated). The molecular weight of each pegylated peptide evaluated is indicated *below* the columns. Tumor uptake was higher for specific *versus* control peptide ($P < 0.001$), and for specific peptide, tumor uptake was increased with increased molecular weight ($P = 0.03$). Control peptide uptake by tumor was not increased with increasing molecular weight (see also Table 5, increase per molecular size). Uptake by kidney and liver was also notably different for specific *versus* control, with higher kidney uptakes observed for control peptides at both 24 and 48 h (with a negative association with molecular weight). In contrast, liver uptake was lower for control peptide compared with specific peptide at 24 h.

of radiolabeled pegylated peptide. A statistically significant interaction for the ANCOVA model ($P < 0.01$) was observed for all organs, except blood, at 24 h, indicating that specific and control uptakes were different. Increased uptake by tumor of specific over control peptide was observed for all sizes of pegylated peptide compared at both 24 and 48 h after injection, demonstrating greater avidity of specific peptide for this lymphoma target (Fig. 3). For example, uptake by tumor of M_r 150,000 specific peptide at 24 h was 13.8 ± 1.0% ID/g (mean ± SD) compared with 3.5 ± 1.3 for control peptide, resulting in a specific/control ratio of 4.0 (Table 3). Tumor uptake was elevated for specific compared with control peptides at 48 h (8.31 ± 2.12 *versus* 2.33 ± 0.45% ID/g M_r 100,000; 10.38 ± 1.94 *versus* 3.38 ± 0.64% ID/g, respectively), and the highest mean tumor/blood ratio (Table 3) associated with the specific M_r 100,000 peptide occurred at 48 h [1.2 ± 0.2 (mean ± SD) *versus* 0.3 ± 0.03 for control peptide], with values decreased for both peptides as blood concentration remained elevated (7.1 ± 1.2% ID/ml, M_r 100,000 specific; 7.24 ± 0.96% ID/ml M_r 100,000 control). However, specific and control blood concentrations were not different at either 24 h or 48 h. In addition to differences in tumor uptake, the change in proline and aspartate isomers between the specific and control peptides resulted in significant differences in kidney and liver uptake at 24 h, but only the uptake in kidney remained different by 48 h. Kidney uptake (% ID/g) ranged from 15.4 ± 1.2 (M_r 70,000) to 7.9 ± 0.4 (M_r 150,000) for specific peptides and 60.0 ± 2.8 (M_r 70,000) to 15.0 ± 1.5 (M_r 150,000) for control peptides at 24 h. As opposed to kidney uptake, liver uptake was increased for specific peptides compared with the control peptides at 24 h (21.4 ± 3.4% ID/g for specific M_r 150,000 peptide compared with 9.6 ± 0.8 for M_r 150,000 control peptide). However, the

Table 3 Specific/control and tumor/normal ratios for organ uptake

Specific to control ratios for key organs were obtained by dividing the mean organ uptake (%ID/g) for specific peptide by the mean organ uptake of control peptide (%ID/g). The number of animals used to evaluate uptake in each group is shown in parentheses. Ratios equal to 1 indicate similar uptake for specific and control peptides, whereas ratios greater than 1 indicate higher uptake for the specific peptide. A tumor/normal tissue ratio was determined for each mouse, and the results from the groups of mice were used to determine the mean ± SD for each organ ratio (Specific M_r 40,000 peptide organ groups had five animals each; control M_r 40,000 peptide organ uptake was not evaluated).

Time (h)	M_r (in thousands)	Organ	Specific/control (*n* specific/*n* control)	Mean specific tumor/normal ± SD	Mean control tumor/normal ± SD
24	70	Tumor	2.0 (5/4)		
		Blood	1.0 (5/4)	0.7 ± 0.1	0.4 ± 0.1
		Kidney	0.3 (5/4)	0.3 ± 0.02	0.04 ± 0.01
		Liver	2.7 (5/5)	0.3 ± 0.1	0.4 ± 0.1
	100	Tumor	2.9 (7/3)		
		Blood	1.1 (9/5)	0.7 ± 0.2	0.3 ± 0.02
		Kidney	0.4 (9/5)	0.8 ± 0.3	0.1 ± 0.02
		Liver	1.6 (9/5)	0.5 ± 0.1	0.3 ± 0.1
	150	Tumor	4.0 (2/4)		
		Blood	1.1 (3/5)	0.7 ± 0.1	0.2 ± 0.1
		Kidney	0.5 (3/5)	1.8 ± 0.04	0.2 ± 0.1
		Liver	2.2 (3/5)	0.7 ± 0.2	0.4 ± 0.1
48	100	Tumor	3.6 (5/5)		
		Blood	1.0 (5/5)	1.2 ± 0.2	0.3 ± 0.03
		Kidney	0.2 (5/5)	1.3 ± 0.3	0.1 ± 0.01
		Liver	0.9 (5/5)	0.6 ± 0.1	0.1 ± 0.02
	150	Tumor	3.1 (4/4)		
		Blood	0.9 (4/4)	1.0 ± 0.2	0.3 ± 0.1
		Kidney	0.3 (4/4)	0.2 ± 0.1	0.2 ± 0.04
		Liver	1.1 (4/4)	0.7 ± 0.1	0.2 ± 0.1

Table 4 Increase per molecular size of specific and control pegylated peptides at 24 and 48 h

Organ uptake increases associated with molecular size were measured as the estimated slopes determined from the regression analysis of individual mouse data using %ID/g *versus* molecular weight of the peptide at 24 or 48 h. Statistical analysis was used to determine whether the slopes were different from zero. Group values are expressed as the estimated slope ± SE. Positive slopes indicate the organ uptake increased with molecular weight (*e.g.*, liver), whereas negative slopes indicate organ uptake decreased with molecular size (such as seen in kidney).

	Slope = increase per M_r size estimated slope ± SE (*P* value)			
	24 h		48 h	
Organ	Specific	Control	Specific	Control
Liver	0.12 ± 0.02 (<0.001)	0.04 ± 0.01 (0.004)	0.03 ± 0.02 (0.268)	−0.03 ± 0.02 (0.23)
Spleen	0.09 ± 0.01 (<0.001)	0.04 ± 0.01 (0.006)	0.06 ± 0.02 (0.007)	0.05 ± 0.01 (0.003)
Kidney	−0.27 ± 0.04 (<0.001)	−0.50 ± 0.09 (<0.001)	−0.02 ± 0.01 (0.134)	−0.27 ± 0.03 (<0.001)
Marrow	0.07 ± 0.01 (<0.001)	0.04 ± 0.01 (<0.001)	0.04 ± 0.03 (0.201)	0.01 ± 0.01 (0.55)
Tumor	0.09 ± 0.01 (<0.001)	0.01 ± 0.01 (0.130)	0.04 ± 0.03 (0.176)	0.02 ± 0.01 (0.023)

difference in liver uptake for specific *versus* control was not maintained at 48 h.

Effect of Molecular Size. As molecular size increased, more uptake of specific and control peptides was observed in all organs, except by kidney and control tumors (Table 4; Fig. 3). Uptake in all organs, evaluated as a function of molecular size at 24 h, appeared to depend on whether specific or control peptide was used, when assessed by comparing the slopes obtained from regression analysis of %ID/g *versus* M_r, ± SE (*P* for interaction < 0.01). Tumor uptake of specific peptide was dependent on molecular size, with an increase in uptake with higher molecular size estimated at 0.09 ± 0.01 at 24 h ($P < 0.001$) and 0.03 ± 0.01 at 48 h ($P = 0.04$; Fig. 4). Kidney uptake as a function of molecular size decreased with increasing molecular weight for both specific and control peptides [slopes of −0.27 ± 0.04 (specific) and −0.50 ± 0.09 (control); $P < 0.001$]. Except for blood, liver uptake of specific pegylated peptide at 24 h demonstrated the most increase with molecular size (regression analysis slope of %ID/g *versus* M_r, ± SE), with a slope of 0.12 ± 0.02. Blood concentration of specific pegylated peptide (% ID/ml) at 24 h was dependent on molecular size, with an estimated change per increase in molecular size of 0.16 ± 0.01 ($P < 0.01$). By 48 h, there was a continued negative association of kidney uptake with molecular size for control peptides, with fewer animals analyzed at this time point ($P < 0.001$; Table 4), and there was no longer a difference in liver uptake associated with molecular size. Blood concentration still depended on molecular size at 48 h ($P < 0.001$), with an estimated change per unit of 0.09 ± 0.01 with the change in concentration as a function of molecular size still the same for

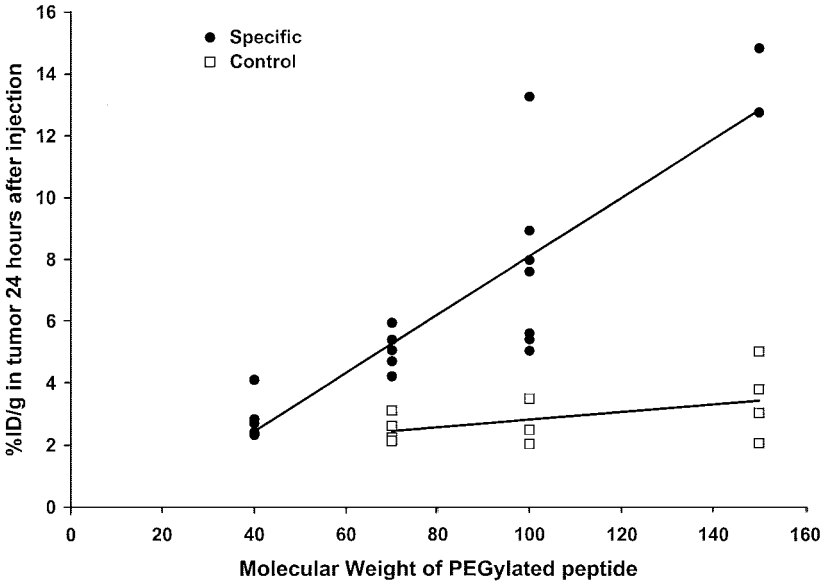

Fig. 4 Tumor uptake of specific and control peptides as a function of pegylated peptide molecular weight. The %ID/g determined at 24 h after injection of pegylated peptide was plotted against the molecular weight of the pegylated peptide injected. Regression analysis was used to describe the slopes of specific and control tumor uptakes *versus* molecular weight (values for other organs in addition to tumors are listed in Table 4) and to determine whether the slopes were different from 0. Specific peptide uptake of tumors at 24 h (●) increased with molecular weight (slope = 0.09 ± 0.01; $P < 0.001$), whereas control peptide uptake (□) did not change with molecular weight (slope = 0.01 ± 0.01; $P = 0.130$).

both peptides (P for interaction = 0.38). For example, blood %ID/ml ± SD for M_r 70,000 specific *versus* control peptide was 7.5 ± 1.2 *versus* 7.2 ± 0.5, respectively, whereas concentration for M_r 150,000 specific *versus* control peptide was 21.2 ± 0.02 *versus* 18.7 ± 1.3% ID/ml, demonstrating the continued influence of molecular size on blood clearance without effect of peptide sequence.

Discussion

The comparisons of clearances and tissue distribution for these specific and control pegylated peptides of multiple matched molecular sizes provide preliminary data important for the development of pegylated tumor targeting therapeutic agents. Whereas it is known that pegylation increases the circulation time of small molecules (23, 25, 27, 30–33, 39, 43, 58–61), the effects on biodistribution are less clear. Unmodified small peptides typically are excreted rapidly, and if they are radiolabeled to a level sufficient to induce tumor response, they frequently have associated renal toxicity (34, 62–65). Thus, knowledge of the behavior of pegylated peptides is vital for developing radiolabeled tumor-targeting therapeutic agents. Currently, pegylation is being investigated as a mechanism to increase both the bioavailability and bioactivity of a number of peptides, including asparaginase, IFN-α, recombinant IL-2, TNF-α, cytokines conjugated to toxin, and photodynamic agents such as chlorin polymers (25, 32, 33, 39, 48, 61, 66). Additionally, pegylation has been studied with tumor targeting antibodies and antibody fragments [Fab, $F(ab')_2$] and single chain antibodies [scFv (27, 35, 42, 46, 47)]. The United States Food and Drug Administration has approved a number of pegylated proteins for imaging (67–71) and therapeutic use (29, 43, 61, 66). In general, pegylation of radiolabeled proteins results in increased molecular size, with decreased glomerular filtration (34, 43, 61, 72). However renal tubular cell and liver hepatocyte uptake compared with nonpegylated proteins may be increased (41, 46–48, 59, 73) or decreased (40, 72, 74) or may remain unchanged (75). Although tumor/normal ratios may increase with pegylation (48), optimal formulations have not been developed for peptide-targeted radionuclide therapy (76), which can potentially provide high tumor delivery with low normal tissue retention.

The precise mechanism by which pegylation increases tumor targeting is not clear, but it has been shown to improve the biological activity of several hormone drugs, cytokines, antibody fragments, and even monoclonal antibodies. This is related to increased circulation time, reduced antigenicity and sensitivity to proteolysis (25), and increased solubility and vascular permeability (26). Pegylation also provides the opportunity to form multidentate versions of peptides and scFv through the use of branched or star PEG polymers, to increase the likelihood of cross-linking with increased binding avidity to tumor cells (31).

Initial studies of the effects of pegylation on clearance and biodistribution of peptides and antibody fragments with linear PEG structures have been reported (23, 25, 31, 33, 46, 77). Compared with the unmodified peptide or antibody fragments, linear pegylated fragments and peptides have prolonged circulation times [$t_{1/2}$ (24, 25, 33, 39, 58, 60)], with resultant increases in tumor uptake and tumor response. Thus, a small protein such as TNF-α has an increased $t_{1/2}$ of 2.25 h compared with 0.047 h when unmodified (33). Increased tumor response has been shown with a number of pegylated peptides, including arginine deiminase (60), IL-2α *Pseudomonas* exotoxin (27), transforming growth factor α *Pseudomonas* exotoxin (39), IL-2 (32, 45), asparaginase (44), and TNF-α (33). Increasing the molecular weight with increased modification by PEG has been shown to decrease clearance (23, 27, 30, 32, 33, 60, 61, 72) and even allow the prediction of clearance times based on molecular weight (23). For example, by increasing the effective molecular weight of pegylated recombinant IL-2 from M_r 40,000 to M_r 208,000, there was a >8-fold increase in the slow phase ($t_{1/2}$-β) of plasma clearance (23). The IL-2 study also illustrated the sharp decrease in clearance for molecular weights above 70,000 (23), above which proteins are excluded from glomerular filtra-

tion by the kidney (34). The decreased clearance with increased molecular weight can result in prolonged increases in %ID in blood. Blood levels close to or over 10% have been reported after pegylation for $F(ab')_2$ (35, 47) at 24 h and for pegylated peptides at 16 h (32). Thus, although tumor uptake may increase as a result of pegylation, the tumor/normal blood ratio may be low and may even be <1 (47), although tumor/blood ratios of 11.9 have been reported for $F(ab')_2$ (35).

Typically, pegylation increases the area under the concentration-time curve in all tissues (46), with increases in liver uptake and kidney uptake seen after pegylation of Fab (46), $F(ab')_2$ (47), or peptides (59, 73). However, depending on the agent, tumor uptake can be increased above that of normal tissues with resultant tumor/normal ratios above 1 (31, 35, 48, 77). Increased tumor/normal tissue ratios of >3 have been reported after pegylation of $F(ab')_2$ anti-carcinoembryonic antigen antibody for kidney and liver (47).

In the study described here, we used a synthetic combinatorial peptide library approach to identify the tumor-targeting sequence *Dhb*-pLDI (15, 16). This peptide binds preferentially to human T- and B-lymphoma cell lines, including Jurkat and Raji, via the $\alpha_4\beta_1$ integrin (16). This integrin is expressed on normal monocytes, lymphocytes, eosinophils, basophils, and macrophages, (78), but the tumor-targeting peptide *Dhb*-pLDI does not bind normal peripheral mononuclear cells (16). Because the stereospecificity of D-proline and L-aspartate is critical for $\alpha_4\beta_1$ integrin binding (16), the control peptide with proline and aspartate stereo isomers *Dhb*-PLdl was used to compare cell binding, pharmacokinetics, and biodistribution. Our *in vitro* results indicate that the control peptide does have some Raji cell binding but does not recognize the same binding site as the specific peptide because they were not competitive.

The *in vivo* results comparing specific with control pegylated peptide indicate that the sequence of the peptide was critical not only for tumor uptake but also for body clearance rate and uptake by key organs (*e.g.*, increased uptake by kidney of control peptide and increased uptake by liver, spleen, and marrow of specific peptide). Definitive explanations for the difference in uptake by normal tissue of specific *versus* control peptides are not possible. Substitution of L for D amino acid should not alter the charge of the molecule, a factor important in kidney uptake (34, 79). However, the negatively charged aspartate could be less accessible in the control molecule than in the specific molecule, resulting in an apparent decrease in negative charge and an increase in uptake by kidney proximal tubular cells (34). Alternatively, the control peptide could potentially bind to some molecule that is more highly expressed on kidney cells than the target of the specific peptide, the $\alpha_4\beta_1$ integrin.

The smallest molecules (M_r 40,000) demonstrated both fast blood clearance and markedly high kidney uptake. Although blood clearance decreased with molecular weight, a clear cutoff at M_r 70,000 from loss of glomerular filtration, as has been reported in rabbits, rats, and mice (23, 30, 80–82), was not discernible from this data. The $t_{1/2}$ of ~5.5 h calculated for the M_r 40,000 specific and control peptides appears longer than other plasma $t_{1/2}$ values typically reported for this size molecule. Knauf *et al.* (23) reported a $t_{1/2}$ (slow phase) of 44 min for a M_r 40,000 pegylated recombinant IL-2 protein; Wang *et al.* (39) reported a $t_{1/2}$ of 80 min (slow phase) for a M_r 135,000 pegylated transforming growth factor α peptide; and Tsutsumi *et al.* (33) reported a $t_{1/2}$ of 0.625 h for a M_r 84,000 pegylated peptide (TNF-α). Thus our predicted clearance times for low molecular weight peptides seem slower in comparison.

In summary, this study illustrates that blood and body clearances of tumor-targeting pegylated peptides and thus tumor uptake can be controlled by varying the molecular size of the PEG. It also illustrates that uptake of pegylated peptides by normal tissues appears to be determined partly by molecular target and partly by subtle differences in available charge or molecular shape, in addition to molecular size. Thus, this study provides unique data emphasizing a need to carefully consider effect of pegylation on normal tissue uptake, beyond the effect of molecular weight. The use of PEG polymers combined with high-affinity tumor cell binding ligands offers a flexible approach to optimize the molecular size and structure for enhanced tumor delivery, tumor binding, and normal tissue clearance, as part of tumor targeting drug development. The information derived from this study provides the basis for such development and characterization of pegylated molecules for systemic tumor targeting radiotherapy.

Acknowledgments

We gratefully acknowledge David L. Kukis, Laird A. Miers, Bonnie Bradt, and Cheng-Yi Xiong, for experimental contributions.

References

1. Goldenberg, D. M. Targeted therapy of cancer with radiolabeled antibodies. J. Nucl. Med., *43:* 693–713, 2002.

2. Knox, S. J., and Meredith, R. F. Clinical radioimmunotherapy. Semin. Radiat. Oncol., *10:* 73–93, 2000.

3. Buchsbaum, D. J. Experimental radioimmunotherapy. Semin. Radiat. Oncol., *10:* 156–167, 2000.

4. Buchsbaum, D. J. Experimental approaches to increase radiolabeled antibody localization in tumors. Cancer Res., *55:* 5729s–5732s, 1995.

5. DeNardo, S. J., Cagnoni, P. J., Wong, J. Y. C., and Richman, C. M. Radionuclide Therapy. *In:* Nuclear Oncology: Diagnosis and Therapy, Section E: Breast Carcinoma, #22, pp. 331–342. New York: Lippincott Williams & Wilkins, 2000.

6. DeNardo, G. L., O'Donnell, R. T., Kroger, L. A., Richman, C. M., Goldstein, D. S., Shen, S., and DeNardo, S. J. Strategies for developing effective radioimmunotherapy for solid tumors. Clin. Cancer Res., *10:* 3219–3223, 1999.

7. DeNardo, S. J. Radioimmunotherapy for breast cancer: systemic tumor-targeted irradiation. Adv. Oncol., *15:* 23–29, 1999.

8. Goshorn, S., Sanderson, J., Axworthy, D., Lin, Y., Hylarides, M., and Schultz, J. Preclinical evaluation of a humanized NR-LU-10 antibody-streptavidin fusion protein for pretargeted cancer therapy. Cancer Biother. Radiopharm., *16:* 109–123, 2001.

9. Dvorak, H. F., Nagy, J. A., and Dvorak, A. M. Structure of solid tumors and the vasculature: implications for therapy with monoclonal antibodies. Cancer Cells, *3:* 77–85, 1991.

10. Shockley, T. R., Lin, K., Nagy, J. A., Tompkins, R. G., Yarmush, M. L., and Dvorak, H. F. Spatial distribution of tumor-specific monoclonal antibodies in human melanoma xenografts. Cancer Res., *52:* 367–376, 1992.

11. Jain, R. K. Delivery of molecular and cellular medicine to solid tumors. Microcirculation, *4:* 1–23, 1997.

12. Thomas, G. E., Esteban, J. M., Raubitschek, A., and Wong, J. Y. γ-Interferon administration after ^{90}yttrium radiolabeled antibody therapy: survival and hematopoietic toxicity studies. Int. J. Radiat. Oncol. Biol. Phys., *31:* 529–534, 1995.

13. Neumeister, P., Eibl, M., Zinke-Cerwenka, W., Scarpatetti, M., Sill, H., and Linkesch, W. Hepatic veno-occlusive disease in two patients with

relapsed acute myeloid leukemia treated with anti-CD33 calicheamicin (CMA-676) immunoconjugate. Ann. Hematol., *80:* 119–120, 2001.

14. Lam, K. S., Salmon, S. E., Hersh, E. M., Hruby, V., Kazmierski, W. M., and Knspp, R. J. A new type of synthetic peptide library for identifying ligand-binding activity. Nature (Lond.), *354:* 82–84, 1991.

15. Lam, K. S., and Zhao, Z. G. Targeted therapy for lymphoma with peptides. Hematol. Oncol. Clin. N. Am., *11:* 1007–1019, 1997.

16. Park, S. I., Renil, M., Vikstrom, B., Amro, N., Song, L-W., Xu, B-L., and Lam, K. S. The use of one-bead one-compound combinatorial library method to identify peptide ligands for α4β1 integrin receptor in non-Hodgkin's lymphoma. Lett. Peptide Sci., *8:* 171–178, 2002.

17. Aina, O. H., Sroka, T. C., Chen, M-L., and Lam, K. S. Therapeutic cancer targeting peptides. Biopolymers, *66:* 184–199, 2002.

18. Kwekkeboom, D. J., Reubi, J. C., Lamberts, S. W. J., Bruining, H. A., Mulder, A. H., Oei, H. Y., and Krenning, E. P. *In vivo* somatostatin receptor imaging in medullary thyroid carcinoma. J. Clin. Endocrinol. Metab., *76:* 1413–1417, 1993.

19. Kwekkeboom, D. J., Krenning, E. P., Bakker, W. H., Oei, H. Y., Kooij, P. P., and Lamberts, S. W. J. Somatostatin analogue scintigraphy in carcinoid tumours. Eur. J. Nucl. Med., *20:* 283–292, 1993.

20. Veronese, F. M. Peptide and protein PEGylation: a review of problems and solutions. Biomaterials, *22:* 405–417, 2001.

21. Zalipsky, S. Functionalized poly(ethylene glycol) for preparation of biologically relevant conjugates. Bioconjug. Chem., *6:* 150–165, 1995.

22. Zalipsky, S., and Menon-Rudolph, S. Hydrazide derivatives of poly-(ethylene glycol) and their bioconjugates. *In:* J. M. Harris and S. Zalipsky (eds.), Poly(ethyleneglycol) Chemistry and Biological applications, pp. 318.–341. Washington DC: American Chemical Society, 1997.

23. Knauf, M. J., Bell, D. P., Hirtzer, P., Luo, Z. P., Young, J. D., and Katre, N. V. Relationship of effective molecular size to systemic clearance in rats of recombinant interleukin-2 chemically modified with water-soluble polymers. J. Biol. Chem., *263:* 15064–15070, 1988.

24. Kozlowski, A., Charles, S. A., and Harris, J. M. Development of pegylated interferons for the treatment of chronic hepatitis C. Biodrugs, *15:* 419–429, 2001.

25. Delgado, C., Francis, G. E., and Fischer, D. Uses and properties of PEG-linked proteins. Crit. Rev. Ther. Drug Carrier Syst., *9:* 249–304, 1992.

26. Francis, G. E., Delgado, C., Fisher, D., Malik, F., and Agrawal, A. K. Poly(ethylene glycol) modification: Relevance of improved methodology to tumour targeting. J. Drug Target., *3:* 321–340, 1996.

27. Tsutsumi, Y., Onda, M., Nagata, S., Lee, B., Kreitman, R. J., and Pastan, I. Site-specific chemical modification with polyethylene glycol of recombinant immunotoxin anti-TAC(FV)-PE38 (LMB-2) improves antitumor activity and reduces animal toxicity and immunogenecity. Proc. Natl. Acad. Sci. USA, *97:* 8548–8553, 2000.

28. Molineux, G. Pegylation: engineering improved pharmaceuticals for enhanced therapy. Cancer Treat. Rev., *28:* 13–16, 2002.

29. Crawford, J. Clinical uses of pegylated pharmaceuticals in oncology. Cancer Treat. Rev., *28:* 7–11, 2002.

30. Koumenis, I. L., Shahrokh, Z., Leong, S., Hsei, V., Deforge, L., and Zapata, G. Modulating pharmacokinetics of an anti-interleukin-8 $F(ab')_2$ by amine-specific pegylation with preserved bioactivity. Int. J. Pharm., *198:* 83–95, 2000.

31. Lee, L. S., Conover, C., Shi, C., Whitlow, M., and Filpula, D. Prolonged circulating lives of single-chain Fv proteins conjugated with polyethylene glycol: a comparison of conjugation chemistries and compounds. Bioconjug. Chem., *10:* 973–981, 1999.

32. Katre, N., Knauf, M. J., and Laird, W. J. Chemical modification of recombinant interleukin 2 by polyetheylene glycol increases its potency in the murine Meth A sarcoma model. Proc. Natl. Acad. Sci. USA, *84:* 1487–1491, 1987.

33. Tsutsumi, Y., Kihira, T., Tsunoda, S., Kamada, H., Nakagawa, S., Kaneda, Y., Kanamori, T., and Mayumi, T. Molecular design of hybrid tumor necrosis factor-α III: polyethylene glycol-modified tumor necrosis factor-α has markedly enhanced antitumor potency due to longer plasma half-life and higher tumor accumulation. J. Pharmacol. Exp. Ther., *278:* 1006–1011, 1996.

34. Behr, T. M., Goldenberg, D. M., and Becker, W. Reducing the renal uptake of radiolabeled antibody fragments and peptides for diagnosis and therapy: present status, future prospects and limitations. Eur. J. Nucl. Med., *25:* 201–212, 1998.

35. Pedley, R. B., Boden, J. A., Boden, R., Begent, R. H. J., Turner, A., Haines, A. M. R., and King, D. J. The potential for enhanced tumour localisation by poly(ethylene glycol) modification of anti-CEA antibody. Br. J. Cancer, *70:* 1126–1130, 1994.

36. Eyre, H. J., and Farver, M. L. Hodgkin's disease and non-Hodgkin's lymphomas. *In:* A. I. Holleb, D. J. Fink, and G. P. Murphy (eds.), Textbook of Clinical Oncology, pp. 377–390. Atlanta, GA: American Cancer Society, 1991.

37. Nucci, M. L., Shorr, R., and Abuchowski, A. The therapeutic value of poly(ethylene glycol)-modified proteins. Adv. Drug Deliv. Rev., *6:* 133–151, 1991.

38. Pettit, D. K., Bonnert, T. P., Eisenman, J., Srinivasan, S., Paxton, R., Beers, C., Lynch, D., Miller, B., Yost, J., Grabstein, K. H., and Gombotz, W. R. Structure-function studies of interleukin 15 using site-specific mutagenesis, poly(ethylene glycol) conjugation, and homology modeling. J. Biol. Chem., *272:* 2312–2318, 1997.

39. Wang, Q-C., Pai, L. H., Debinski, W., FitzGerald, D. J., and Pastan, I. Poly(ethylene glycol)-modified chimeric toxin composed of transforming growth factor α and *Pseudomonas* exotoxin. Cancer Res., *53:* 4588–4594, 1993.

40. Wen, X., Wu, Q., Ke, S., Ellis, L., Charnsangavej, C., Delpassand, A. S., Wallace, S., and Li, C. Conjugation with ^{111}In-DTPA-poly(ethylene glycol) improves imaging of anti-EGF receptor antibody C225. J. Nucl. Med., *42:* 1530–1537, 2001.

41. Deckert, P. M., Jungbluth, A., Montalto, N., Clark, M. A., Finn, R. D., Williams, C. J., Richards, E. C., Panageas, K. S., Old, L. J., and Welt, S. Pharmacokinetics and microdistribution of polyethylene glycol-modified humanized A33 antibody targeting colon cancer xenografts. Int. J. Cancer, *87:* 382–390, 2000.

42. Kitamura, K., Takahashi, T., Yamaguchi, T., Noguchi, A., Takashina, K-I., Tsurumi, H., Inagake, M., Toyokuni, T., and Hakomori, S-I. Chemical engineering of the monoclonal antibody A7 by polyethylene glycol for targeting cancer chemotherapy. Cancer Res., *51:* 4310–4315, 1991.

43. Yowell, S. L., and Blackwell, S. Novel effects with polyethylene glycol modified pharmaceuticals. Cancer Treat. Rev., *28:* 3–6, 2002.

44. Abuchowski, A., Kazo, G. M., Verhoest, C. R., Jr., van Es, T., Kafkewitz, D., Nucci, M. L., Viau, A. T., and Davis, F. F. Cancer therapy with chemically modified enzymes. I. Antitumor properties of polyethylene glycol-asparaginase conjugates. Cancer Biochem. Biophys., *7:* 175–186, 1984.

45. Zimmerman, R. J., Aukerman, S. L., Katre, N. V., Winkelhake, J. L., and Young, J. D. Schedule dependence of the antitumor activity and toxicity of polyethylene glycol-modified interleukin-2 in murine tumor models. Cancer Res., *49:* 6521–6528, 1989.

46. Delgado, C., Pedley, R. B., Herraez, A., Boden, R., Boden, J. A., Keep, P. A., Chester, K. A., Fisher, D., Begent, R. H. J., and Francis, G. E. Enhanced tumour specificity of anti-carcinoembryonic antigen Fab′ fragment by poly(ethylene glycol) (PEG) modification. Br. J. Cancer, *73:* 175–182, 1996.

47. Eno-Amooquaye, E. A., Searle, F., Boden, J. A., Sharma, S. K., and Burke, P. J. Altered biodistribution of an antibody-enzyme conjugate modified with polyethylene glycol. Br. J. Cancer, *73:* 1323–1327, 1996.

48. Hamblin, M. R., Miller, J. L., Rizvi, I., Ortel, B., Maytin, E. V., and Hasan, T. Pegylation of a chlorin$_{e6}$ polymer conjugate increases tumor targeting of photosensitizer. Cancer Res., *61:* 7155–7162, 2001.

49. Fields, G. B., and Noble, R. L. Solid phase peptide synthesis utilizing 9-fluorenylmethoxycarbonyl amino acids. Int. J. Pept. Protein Res., *35:* 161–214, 1990.

50. Kaiser, E., Colescott, R. L., Bossinger, C. D., and Cook, P. I. Color test for detection of free terminal amino groups in the solid-phase synthesis of peptides. Anal. Biochem., *34:* 595–598, 1970.

51. DeNardo, S. J., Kukis, D. L., Miers, L. A., Winthrop, M. D., Kroger, L. A., Salako, Q., Shen, S., Lamborn, K. R., Gumerlock, P. H., Meares,

C. F., and DeNardo, G. L. Yttrium-90-DOTA-peptide-chimeric L6 radioimmunoconjugate: efficacy and toxicity in mice bearing p53 mutant human breast cancer xenografts. J. Nucl. Med., *39:* 842–849, 1998.

52. Penefsky, H. S. A centrifuged-column procedure for the measurement of ligand binding by beef heart F1. Methods Enzymol., *56G:* 527–530, 1979.

53. Kukis, D. L., DeNardo, G. L., DeNardo, S. J., Mirick, G. R., Miers, L. A., Greiner, D. P., and Meares, C. F. Effect of the extent of chelate substitution on the immunoreactivity and biodistribution of 2IT-BAT-Lym-1 immunoconjugates. Cancer Res., *55:* 878–884, 1995.

54. DeNardo, G. L., DeNardo, S. J., Wessels, B. W., Kukis, D. L., Miyao, N., and Yuan, A. ^{131}I-Lym-1 in mice implanted with human Burkitt's lymphoma (Raji) tumors: loss of tumor specificity due to radiolysis. Cancer Biother. Radiopharm., *15:* 547–560, 2000.

55. Lin, K., Ateeq, H. S., Hsiung, S. H., Chong, L. T., Zimmermann, C. N., Castro, A., Lee, W., Hammond, C. E., Kalkunte, S., Chen, L., Pepinsky, R. B., Leone, D. R., Sprague, A. G., Abraham, W. M., Gill, A., Lobb, R. R., and Adams, S. P. Selective, tight-binding inhibitors of integrin $\alpha_4\beta_1$ that inhibit allergic airway responses. J. Med. Chem., *42:* 920–934, 1999.

56. Scatchard, G. The attraction of proteins for small molecules and ions. Ann. N. Y. Acad. Sci., *51:* 660–666, 1947.

57. DeNardo, G. L., Kukis, D. L., Shen, S., Mausner, L. F., Meares, C. F., Srivastava, S. C., Miers, L. A., and DeNardo, S. J. Efficacy and toxicity of ^{67}Cu-2IT-BAT-Lym-1 radioimmunoconjugate in mice implanted with Burkitt's lymphoma (Raji). Clin. Cancer Res., *3:* 71–79, 1997.

58. Pepinsky, R. B., Lepage, D. J., Gill, A., Chakraborty, A., Vaidyanathan, S., Green, M., Baker, D. P., Whalley, E., Hochman, P. S., and Martin, P. Improved pharmacokinetic properties of a polyethylene glycol modified form of interferon-β-1a with preserved *in vitro* bioactivity. J. Pharmacol. Exp. Ther., *297:* 1059–1066, 2001.

59. Pepinsky, R. B., Shapiro, R. I., Wang, S., Chakraborty, A., Gill, A., Lepage, D. J., Wen, D., Rayhorn, P., Horan, G. S. B., Taylor, F. R., Garber, E. A., Galdes, A., and Engber, T. M. Long-acting forms of sonic hedgehog with improved pharmacokinetic and pharmacodynamic properties are efficacious in a nerve injury model. J. Pharm. Sci., *91:* 371–387, 2002.

60. Ensor, C. M., Holtzberg, F. W., Bomalaski, J. S., and Clark, M. A. Pegylated arginine deiminase (ADI-SS $PEG_{20,000\ mw}$) inhibits human melanomas and hepatocellular carcinomas *in vitro* and *in vivo.* Cancer Res., *62:* 5443–5450, 2002.

61. Luxon, B. A., Grace, M., Brassard, D., and Bordens, R. Pegylated interferons for the treatment of chronic hepatitis C infection. Clin. Ther., *24:* 1363–1383, 2002.

62. Baum, R. P., Niesen, A., Hertel, A., Adams, S., Kojouharoff, G., Goldenberg, D. M., and Hor, G. Initial clinical results with technetium-99m-labeled LL2 monoclonal antibody fragment in the radioimmunodetection of B-cell lymphomas. Cancer (Phila.), *73:* 896–899, 1994.

63. Blumenthal, R. D., Sharkey, R. M. and Goldenberg, D. M. Overcoming dose-limiting, radioantibody-induced myelotoxicity. *In:* D. M. Goldenberg (ed.), Cancer Therapy with Radiolabeled Antibodies, pp. 295–314. Boca Raton, FL: CRC Press, 1995.

64. de Jong, M., Bakker, W. H., Krenning, E. P., Breeman, W. A., van der Pluijm, M. E., Bernard, B. F., Visser, T. J., Jermann, E., Behe, M., Powell, P., and Macke, H. R. Yttrium-90 and indium-111 labelling, receptor binding and biodistribution of [DOTA, S-Phe, Tyr] octreotide, a promising somatostatin analogue for radionuclide therapy. Eur. J. Nucl. Med., *24:* 368–371, 1997.

65. Reubi, J. C. Regulatory peptide receptors as molecular targets for cancer diagnosis and therapy, Q. J. Nucl. Med., *41:* 63–70, 1997.

66. Reddy, K. R., Wright, T. L., Pockros, P. J., Shiffman, M., Everson, G., Reindollar, R., Fried, M. W., Purdum, P. P., Jensen, D., Smith, C., Lee, W. M., Boyer, T. D., Lin, A., Pedder, S., and DePamphilis, J. Efficacy and safety of pegylated (40-kd) interferon α-2α compared with interferon α-2α in noncirrhotic patients with chronic hepatitis C. Hepatology, *33:* 433–438, 2001.

67. Kwekkeboom, D. J., Bakker, W. H., Kooij, P. P. M., Erion, J., Srinivasan, A., de Jong, M., Reubi, J-C., and Krenning, E. P. Cholecystokinin receptor imaging using an octapeptide DTPA-CCK analogue in patients with medullary thyroid carcinoma. Eur. J. Nucl. Med., *27:* 1312–1217, 2000.

68. Reubi, J. C., Lamberts, S. J., and Krenning, E. P. Receptor imaging of human diseases using radiolabeled peptides. J. Recept. Signal Transduct. Res., *15:* 379–392, 1995.

69. Smith-Jones, P. M., Bischof, C., Leimer, M., Gludovacz, D., Angelberger, P., Pangerl, T., Peck-Radosavljevic, M., Hamilton, G., Kaserer, K., Kofler, A., Schlagbauer-Wadl, H., Traub, T., and Virgolini, I. DOTA-lanreotide: a novel somatostatin analog for tumor diagnosis and therapy. Endocrinology, *140:* 5136–5148, 1999.

70. Kwekkeboom, D. J., Kooij, P. P., Bakker, W. H., Macke, H. R., and Krenning, E. P. Comparison of 111In-DOTA-Tyr3-octreotide and 111In-DTPA-octreotide in the same patients: biodistribution, kinetics, organ and tumor uptake. J. Nucl. Med., *40:* 762–767, 1999.

71. Kwekkeboom, D., Krenning, E. P., and de Jong, M. Peptide receptor imaging and therapy. J. Nucl. Med., *41:* 1704–1713, 2000.

72. Arpicco, S., Dosio, F., Bolognesi, A., Lubelli, C., Brusa, P., Stella, B., Ceruti, M., and Cattel, L. Novel poly(ethylene glycol) derivatives for preparation of ribosome-inactivating protein conjugates. Bioconjug. Chem., *13:* 757–765, 2002.

73. Newman, M. S., Colbern, G. T., Working, P. K., Engbers, C., and Amantea, M. A. Comparative pharmacokinetics, tissue distribution, and therapeutic effectiveness of cisplatin encapsulated in long-circulating, pegylated liposomes (SPI-077) in tumor-bearing mice. Cancer Chemother. Pharmacol., *43:* 1–7, 1999.

74. Chinol, M., Casalini, P., Maggiolo, M., Canevari, S., Omodeo, E. S., Caliceti, P., Veronese, F. M., Chiolerio, F., Nardone, E., Siccardi, A. G., and Paganelli, G. Biochemical modifications of avidin improve pharmacokinetics and biodistribution, and reduce immunogenicity. Br. J. Cancer, *78:* 189–197, 1998.

75. Fang, J., Sawa, T., Akaike, T., and Maeda, H. Tumor-targeted delivery of polyethylene glycol-conjugated D-amino acid oxidase for antitumor therapy via enzymatic generation of hydrogen peroxide. Cancer Res., *62:* 3138–3143, 2002.

76. Virgolini, I., Traub, T., Novotny, C., Leimer, M., Fuger, B., Li, S. R., Patri, P., Pangerl, T., Angelberger, P., Rederer, M., Andreae, F., Kurtaran, A., and Dudczak, R. New trends in peptide receptor radioligands, Q. J. Nucl. Med., *45:* 153–159, 2001.

77. Wang, M., Lee, L. S., Nepomich, A., Yang, J-D., Conover, C., Whitlow, M., and Fipula, D. Single-chain Fv with manifold *N*-glycans as bifunctional scaffolds for immunomolecules. Protein Eng., *11:* 1277–1283, 1998.

78. Jackson, D. Y. [Alpha]-4 Integrin antagonists. Curr. Pharm. Des., *8:* 1229–1253, 2002.

79. Kobayashi, H., Le, N., Kim, I-S., Kim, M-K., Pie, J-E., Drumm, D., Paik, D. S., Waldmann, T. A., Paik, C. H., and Carrasquillo, J. A. The pharmacokinetic characteristics of glycolated humanized anti-tac Fabs are determined by their isoelectric points. Cancer Res., *59:* 422–430, 1999.

80. Hamano, Y., Grunkemeyer, A., Sudhakar, A., Zeisberg, M., Cosgrove, D., Morello, R., Lee, B., Sugimoto, H., and Kalluri, R. Determinants of vascular permeability in the kidney glomerulus. J. Biol. Chem., *277:* 31154–31162, 2002.

81. Rodewald, R., and Karnovsky, M. J. Porous structure of the glomerular slit diaphragm in the rat and mouse. J. Cell Biol., *60:* 423–433, 1974.

82. Caulfield, J. P., and Farquhar, M. G. The permeability of glomerular capillaries to graded dextrans. J. Cell Biol., *63:* 883–903, 1974.